Journal of Functional Foods 120 (2024) 106390

Contents lists available at ScienceDirect

Journal of Functional Foods

journal homepage: www.elsevier.com/locate/jff

Compound probiotics and glycyrrhizic acid alleviate DON-induced liver damage linked to the alteration of lipid metabolism in piglets

Mengjie Liu [a,b,1], Guorong Yan [a,1], Juan Chang [b], Ping Wang [b], Chaoqi Liu [b], Qingqiang Yin [b,c,*], Xiaoxiang Xu [a,b,*]

[a] Shanghai Skin Disease Hospital, School of Medicine, Tongji University, Shanghai 200443, China
[b] College of Animal Science and Technology, Henan Agricultural University, Zhengzhou 450046, China
[c] Henan Delin Biological Product Co. Ltd., Xinxiang 453000, China

ARTICLE INFO

Keywords:
Deoxynivalenol
Compound probiotics
Glycyrrhinic acid
Liver
Piglets
Lipid metabolism

ABSTRACT

Compound probiotics are capable of effectively breaking down mycotoxins, and glycyrrhizic acid (GA) exhibits hepatoprotective properties. However, the protective efficacy and the underlying mechanism of combined intervention of GA and probiotics (GAP) on ameliorating Deoxynivalenol (DON)-induced liver toxicity remains unclear. This experiment involved 120 weaned piglets, encompassing the control group, the DON group, and the GPD group (*E. faecalis* and *S. cerevisiae* + GA + DON). Results showed that GAP significantly mitigated DON-related liver damage and oxidative stress. Furthermore, GAP inhibited the Nrf2/MAPK/NF-κB pathway, ultimately decreasing liver inflammation and apoptosis. Additionally, GAP significantly enhanced the expressions of ZO-1, GLUT2, PePT1, ASCT2, Occludin and Claudin-1. Moreover, metabolomics analysis revealed that GAP modulated lipid metabolism and mitigated liver damage by elevating serum levels of metabolites, such as phosphatidylcholine, phosphatidylethanolamine, and 3-amino-4-hydroxybenzoic acid. The research provides a theoretically based framework for using GAP to combat DON-induced hepatotoxicity in piglets.

1. Introduction

The fungal secondary metabolite, mycotoxin, often contaminates cereal grains and has become a significant threat to the health of humans and animals (Zhao et al., 2021). Deoxynivalenol (DON), also commonly called vomitoxin, is a prevalent mycotoxin in agricultural products, primarily generated by the *Fusarium cerealis*, *Fusarium culmorum*, and *Fusarium graminearum* (Ma et al., 2018; Maresca, 2013). Since its high contamination rate and toxicity, DON has become a pressing global issue. DON is remarkably stable throughout feed processing and persists during digestion (Tibola et al., 2016; Zhang et al., 2021). Pig is particularly susceptible to DON, as it can distribute widely throughout their body fluids and various organs, compromising intestinal barrier integrity, escalating intestinal inflammation, and disrupting the balance of gut microbiota (Chen et al., 2019; Tang et al., 2021; Xu et al., 2023). The liver, as the metabolic hub in the body, executes diverse physiological functions, including bile synthesis, lipid metabolism, phagocytosis, detoxification, and defense (Liu et al., 2020). Due to the hepatic functions are complex and diverse, making the hepatic highly vulnerable to toxic insults. Recent researches have shown that liver is a principal target organ to the DON exposure (Hu et al., 2023; Ji et al., 2023; Woelflingseder et al., 2018). Therefore, the hepatotoxicity induced by DON is receiving increasing attention.

The liver toxicity caused by DON is primarily attributed to the inflammation, apoptosis, and oxidative stress (Hasuda et al., 2022; Ji et al., 2023; Mao et al., 2022). The crucial of involvement of nuclear factor κB (NF-κB) and mitogen-activated protein kinase (MAPK) signaling pathways in liver inflammation has been demonstrated in various studies (Feng et al., 2023; Jia et al., 2021; Li et al., 2022). DON could elevate the reactive oxygen species (ROS) level and reduces antioxidant enzyme activity, inhibiting the Nrf2 pathway to produce oxidative stress, and activating the MAPK pathway to induce liver inflammation (Hu et al., 2023). ROS can also activate NF-κB signaling pathway, resulting in the generation of pro-inflammatory cytokines (Wang et al., 2021). Consequently, there is an urgent need for anti-inflammatory and antioxidant agents to effectively reduce DON-

* Corresponding authors at: Shanghai Skin Disease Hospital, School of Medicine, Tongji University, Shanghai 200443, China (X. Xu); College of Animal Science and Technology, Henan Agricultural University, Zhengzhou 450046, China (Q.Yin).
E-mail addresses: qqy1964@henau.edu.cn (Q. Yin), xiaoxiangxu@tongji.edu.cn (X. Xu).
[1] The contribution of these authors to this work is equal.

https://doi.org/10.1016/j.jff.2024.106390
Received 20 May 2024; Received in revised form 20 July 2024; Accepted 31 July 2024
Available online 6 August 2024

induced hepatotoxicity.

Glycyrrhizic acid (GA), a natural extract of the Chinese herb liquorice, was shown to alleviate inflammation, oxidative stress and apoptosis (Wang et al., 2022). Meanwhile, GA is also recognized as an effective treatment for liver diseases (Yuan et al., 2019). Additionally, *Lactobacillus* spp. (de Souza et al., 2020) and compound probiotics (Wang et al., 2022) can effectively degrade mycotoxins and alleviate liver damage and oxidative stress induced by DON. Our previous in vivo experiments have demonstrated that the combination of compound probiotics (*S. cerevisiae* and *E. faecalis*) and GA (GAP) can effectively promote the degradation of DON, counteract its inhibitory effects on growth, alleviate intestinal apoptosis and inflammation, regulate nutrient absorption and transport, improve intestinal barrier function, and mitigate DON-induced injury (Xu et al., 2023; Xu et al., 2023). Nevertheless, the protective effect of GAP for DON-related liver damage in weaned piglets remains unclear. In recent years, metabolomics has been widely applied in toxicological analysis, drug development and disease diagnosis (Panisson et al., 2023; Saia et al., 2019; Yang et al., 2020). Nevertheless, the metabolic alterations in liver induced by DON remain poorly understood.

Hence, this study evaluates the protective effect of GAP against DON exposure on liver damage in weaned piglets. We studied the effects of GAP on liver damage, inflammation, apoptosis, oxidative stress, barrier function, and nutrient transport function. Subsequently, we further explored serum metabolites based on metabolomics. Our results will offer foundational evidence regarding the protective efficacy and underlying mechanisms of GAP against DON-mediated liver injury, thereby aiding in the advancement of novel feed additives.

2. Materials and methods

2.1. Animals and experimental design

The animal experimental protocols in this research adhered to the Chinese Guidelines for Institutional Animal Welfare and were authorized by the Animal Care and Use Committee of Henan Agricultural University (SKLAB-B-2010–003–01).

For this experiment, 120 weaned piglets (42-day-old, Landrace × Large White crossbred) were utilized. All weaned piglets were kept in environment-controlled pens and had unimpeded diet and water availability during the entire 28-day experimental period. After acclimatization for one week, all piglets were assigned at random to three groups (with 4 piglets/pen and 10 pens/treatment, half male and half female): the CON group, which fed a basal diet, the DON group, which fed a DON-contaminated moldy diet (1040 μg/kg DON), the GPD group, which fed a DON-contaminated moldy diet with supplementation of GAP (1×10^6 CFU/g *E. faecalis* and *S. cerevisiae* + 400 mg/kg GA). *E. faecalis* (CGMCC1.2135), *S. cerevisiae* (CGMCC 2.1542), GA (95 % purity) and moldy wheat were supplied by Henan Delin Biological Products Co. Ltd., China. The moldy diet was determined to contain 1040 μg/kg DON, and other mycotoxins were detected below the quantification limit. The dosages of DON or GAP were according to previous research (Xu et al., 2023).

At the conclusion of the experiment, three castrated piglets per group were sacrificed. The external jugular vein was used to draw blood samples in clotting accelerator tubes. After centrifugation at 3,000 × g for 10 min at 4 °C, the supernatant was collected and then stored at −20 °C for future use. After a normal saline wash, 1.0 cm^3 of liver was chosen and preserved in 4 % paraformaldehyde for subsequent histological examination. The remaining liver tissue was removed aseptically, frozen in liquid nitrogen right away and kept at −80 °C for further examination.

2.2. Histopathology analysis

Liver tissues were fixed with 4 % paraformaldehyde, dehydrated, paraffin-embedded, and then sectioned for hematoxylin-eosin (H&E) staining. Finally, the sections were then scanned by using a high-resolution automatic digital slice scanning system.

2.3. Detection of serum antioxidant levels and inflammatory cytokines

Blood samples of piglets were conducted by 3,000 × g for 15 min at 4 °C, and the supernatant was stored in −20 °C refrigerator for later biochemical analysis. The antioxidant indicators were measured in the serum and liver of piglets by spectrophotometrically using ELISA kits (Beijing Solarbio Science & Technology Co., Ltd, Beijing, China) following the manufacturer's protocols. The serum levels of IL-8, NF-κB and Caspase 3 in piglets were evaluated through ELISA kits in accordance with the manufacturer's recommended protocols (Jiangsu Meimian Industrial Co., Ltd., Jiangsu, China).

2.4. Quantitative RT-PCR analysis

Total RNA for each liver tissue was extracted by Trizol reagent (Takara, Dalian, China) following the manufacturer's recommendations. First-strand cDNA synthesis was performed using StarScript II First-strand cDNA Synthesis Mix (TaKaRa, Dalin, China). qRT–PCR amplification was carried out on a CFX Connect™ Real-Time PCR Detection System (BioRad, Hercules, CA, USA) with SYBR Green PCR Master Mix (Takara, Dalian, China). The relative mRNA expression levels of genes were standardized with GAPDH according to the $2^{-\Delta\Delta Ct}$ method. All the primers used in the present study were listed as described in our previous study (Xu et al., 2020).

2.5. Western blot analysis

The liver sample was treated with RIPA buffer to lyse it, followed by measuring the protein concentrations. Next, the western blotting was conducted as already reported (Xu et al., 2020). Membranes were allowed to incubate overnight at 4 °C with the appropriate primary antibodies, and then exposed to secondary antibodies (Goat anti-rabbit IgG, CST, USA) for 2 h at room temperature. The primary antibodies used in the protein blots included anti-COX-2 (abs120547), anti-TNF-α (abs123966), anti-Bcl-2 (CST, USA), anti-Bax (CST, USA), anti-ZO-1 (21773–1-AP, Protein-tech), anti-Claudin-1 (13050–1-AP, Protein-tech), anti-Occludin (27260–1-AP, Protein-tech), anti-SOD2 (CST, USA), anti-Nrf2 (CST, USA), anti-NQO1 (CST, USA), anti-HO-1 (CST, USA), anti-phospho-ERK (CST, USA), anti-phospho-JNK (CST, USA), anti-phospho-p38 (CST, USA), anti-p38 (CST, USA), anti-ERK (CST, USA), anti-JNK (CST, USA), anti-phospho-NF-κB (CST, USA) and anti-GAPDH (CST, USA) were acquired on ChemiDOCTM Imaging System (BIO-RAD, USA).

2.6. Serum metabolomic analysis

Based on published literature, metabolites were extracted from serum samples in accordance with established methods (Liu et al., 2024). The serum sample was mixed with extraction solution contained an internal standard (1000:2 vol ratio) consisting of methanol and acetonitrile (1:1). Afterward, the blend underwent centrifugation, and the liquid above the sediment was evaporated, followed by reconstitution in a solution containing 50 % acetonitrile.After another round of centrifuged, the supernatant was transferred to an UPLC-MS sample vial with microtube for subsequent UPLC-MS analysis.

A positive and a negative ion mode of analysis was performed on all samples. Solvents A (0.1 % formic acid) and B (0.1 % formic acid in acetonitrile) were employed in the elution mode. Gradient elution was carried out according to the following conditions: 98 % A and 2 % B for 0.25 min, then 2 % A and 98 % B for 12.75 min, and lastly 98 % A and 2 % for 1.9 min. The acquisition software (MassLynx V4.2, Waters) managed the mass spectrometric parameter settings, enabling the

simultaneous acquisition of dual-channel low and high collision energy data. The collision energy ranged from 2 to 40 V, with a scanning frequency of 0.2 s for each mass spectrum. The IDA approach was utilized for the detection of potential biomarkers in positive and negative ionization modes.

The obtained mass spectral information, including the nuclear-to-mass ratio M/s, dwell time and ionic strength of the substances, were collected and analyzed by Masslynx software onboard the instrument to obtain the quantitative data for all markers in each sample. Subsequently, the data were imported into Simca 13.0 software for multivariate statistical analysis. Various groups were distinguished based on metabolic differences through the reduction and categorization of multidimensional data using techniques such as principal component analysis (PCA) and partial least squares discriminant analysis (PLS-DA). According to the variable projection importance (VIP) of compounds and combined with biological significance, compounds with the largest difference between groups were identified as a potential biomarker. When VIP > 1 and $P < 0.05$, metabolites were considered statistically significant. The validity of these potential biomarkers was confirmed through comparison of their MS/MS spectra and searching databases like HMDB (http//https://www.hmdb.ca/) and KEGG (http//https://www.genome.jp/keg/) for metabolite details. The metabolic pathway analysis was then conducted to investigate the biological processes associated with the differentially expressed metabolites.

2.7. Statistical analysis

All quantified data was represented using the mean ± standard deviation (SD). Statistical analysis was conducted with the SPSS 22.0 software. Normality was checked using the Shapiro-Wilk test and the significance of difference between two groups was calculated by Student's two-sided *t*-tests. The graphs were created by GraphPad Prism 8. Multiple test correction was carried out using the post-hoc false discovery rate method. The $P < 0.05$ was considered as statistically significant.

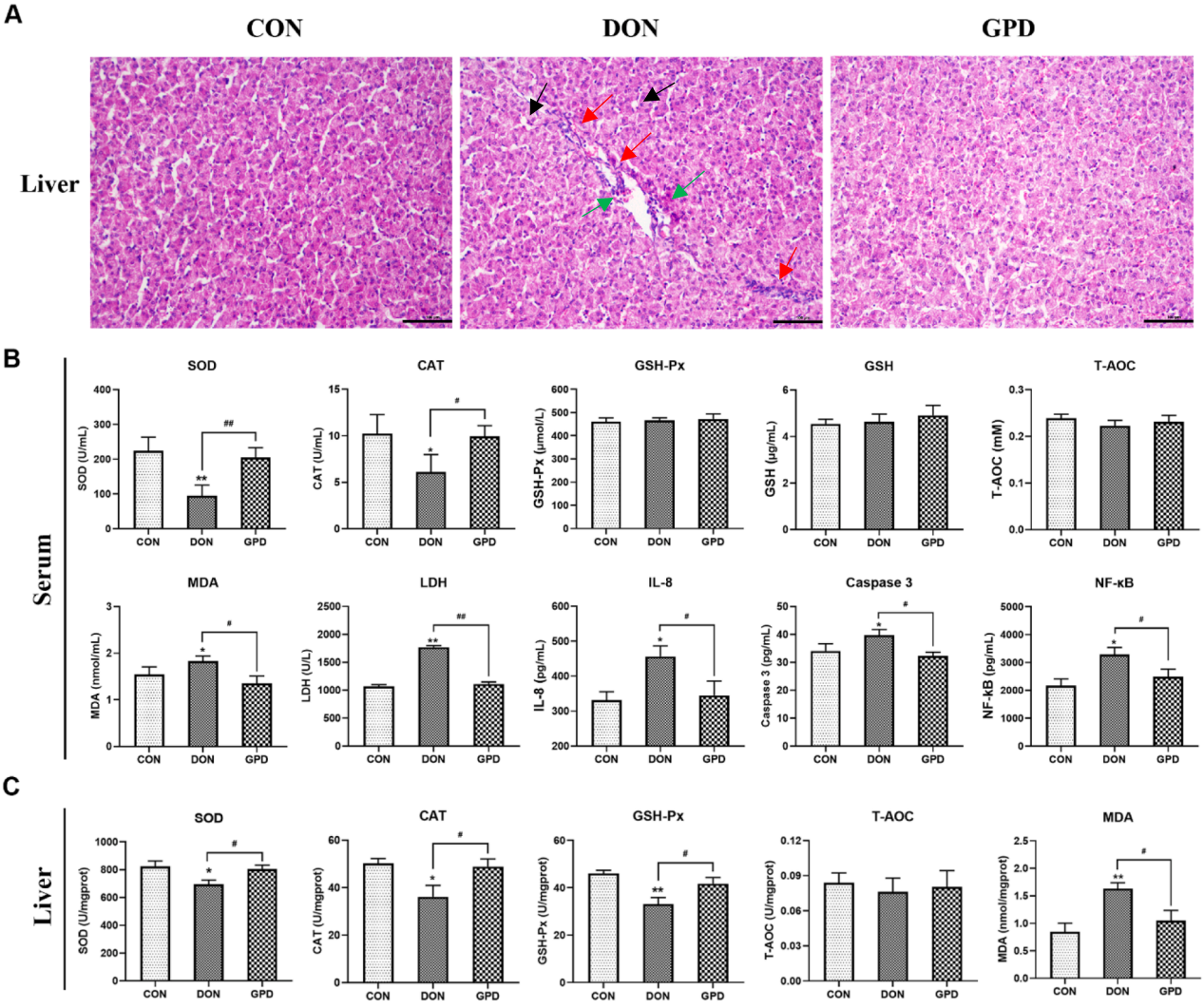

Fig. 1. The impact of GAP on liver histopathological morphology and antioxidant index, IL-8, Caspase 3, NF-κB contents of weaned piglets. (A) Histological characterization in the liver. The red arrows were indicated as infiltrations of lymphocytes and eosinophils, the greens arrows were indicated as individual hepatocyte hemorrhage and necrosis, and the black arrows were indicated as even nuclear lysis and rupture, scale bar = 100 μm. (B) Antioxidant indexes and serum levels of IL-8, Caspase 3 and NF-κB. (C) Antioxidant indexes in the liver. CON: Dietary wheat for the piglets; DON: Dietary wheat for the piglets including 1040 μg/kg DON; GPD: Dietary wheat for the piglets including 400 mg/kg GA, 1×10^6 CFU/g *E. faecalis* and *S. cerevisiae*, 1040 μg/kg DON. * indicates $P < 0.05$, ** indicates $P < 0.01$ relative to the CON group; # indicates $P < 0.05$, ## indicates $P < 0.01$ relative to the DON group.

3. Results

3.1. GAP supplementation ameliorated DON-induced liver damage and oxidative stress

The liver of weaned piglets in the DON group showed serious inflammation, with infiltrations of lymphocytes and eosinophils (red arrow), individual hepatocyte hemorrhage and necrosis (green arrow), and even nuclear lysis and rupture (black arrow) compared to the CON group. In contrast, the GPD group mitigated liver inflammation and prevented the occurrence of hepatocyte bleeding and necrosis **(**Fig. 1**A).** Fig. 1**B** indicated that the activity of serum SOD ($P < 0.01$) and CAT ($P < 0.05$) were markedly decreased and the contents of MDA, LDH ($P < 0.01$), IL-8, Caspase 3 and NF-κB were markedly upregulated ($P < 0.05$) in the DON group compared with the CON group. However, the activities of SOD and CAT in the GPD group were significantly increased compared to the DON group ($P < 0.05$), and the contents of MDA, LDH, IL-8, Caspase 3 and NF-κB in GAP and GPD groups were markedly reduced compared to the DON group ($P < 0.05$). In addition, the DON group markedly suppressed the SOD, CAT ($P < 0.05$) and GSH-Px ($P < 0.01$) activities and markedly increased the MDA content ($P < 0.01$) compared to the CON group. Conversely, compared with the DON group, the GPD group significantly enhanced the activities of SOD, CAT and GSH-Px ($P < 0.05$), and reduced MDA content ($P < 0.05$). No notable variation in T-AOC was observed among the groups ($P > 0.05$) **(**Fig. 1**C).**

3.2. GAP supplementation alleviated liver inflammation and apoptosis in DON-contaminated weaned piglets

The study found that the COX-2 and IL-8 mRNA levels in the DON group were notably upregulated ($P < 0.01$), whereas Bcl-2 mRNA relative expression was substantially downregulated ($P < 0.01$) compared with the CON group. Conversely, the GPD group exhibited a marked decrease in the mRNA relative expression of IL-8, COX-2, and Caspase 3 ($P < 0.05$), and a notable upregulation of the Bcl-2 mRNA relative expression ($P < 0.01$) compared to the DON group. No significant variation was found in the expression of IL-10, TNF-α and Bax among all groups ($P > 0.05$) **(**Fig. 2**A-B).** Fig. 2**C-D** demonstrated that the DON group had a markedly upregulation protein levels of COX-2, TNF-α, Bax ($P < 0.05$), while the Bcl-2 protein was reduced ($P < 0.01$) comparing to CON group. However, the GPD group noticeably enhanced the level of Bcl-2 protein ($P < 0.05$) and decreased levels of Bax, COX-2 and TNF-α proteins ($P < 0.05$) in comparison to DON group.

3.3. GAP supplementation alleviated liver barrier function and transport of nutrients in DON-contaminated weaned piglets

As depicted in Fig. 3**A-D**, compared to the CON group, the DON group markedly reduced the expressions of ZO-1, Occludin and Claudin-1 genes and proteins ($P < 0.05$). In comparison to the DON group, the GPD group markedly raised the expressions of these proteins and genes ($P < 0.05$). Furthermore, compared with the CON group, the mRNA relative expression of GULT2 in the DON group was markedly reduced ($P < 0.01$), whereas adding GAP markedly upregulated the level of GLUT2 ($P < 0.01$). Compare with the DON group, the GPD group notably increased ASCT2 and PePT1 gene levels ($P < 0.05$). Moreover, there was no significant difference in SGLT1 gene expression between the DON and GPD groups ($P > 0.05$).

3.4. GAP supplementation regulated the Nrf2/MAPK/NF-κB pathway in DON-contaminated weaned piglets

As demonstrated in Fig. 4**A-B**, the DON group exhibited markedly decreased protein levels in SOD2, Nrf2, NQO1 and HO-1 compared to the CON group ($P < 0.05$), whereas the GPD group showed a significant increase in these protein levels relative to the DON group ($P < 0.05$). In addition, DON markedly upregulated the expressions of p-JNK and p-ERK ($P < 0.01$), but with no significantly different effect on p-p38 compared to the CON group ($P > 0.05$). GAP addition markedly reduced the expressions of p-JNK and p-ERK ($P < 0.05$). Moreover, DON increased p-NF-κB protein expression and GAP significantly inhibited this increase ($P < 0.05$) (Fig. 4**C-D**).

3.5. GAP supplementation altered serum metabolites in DON-contaminated weaned piglets

To investigate the impact of DON and GPD on the metabolism of weaned piglets, we conducted a non-targeted metabolomics analysis was conducted on nine serum samples from each group. The metabolomics data revealed that each group showed satisfactory stability and repeatability, with PC1 and PC2 explained 67.46 % and 26.40 % of the

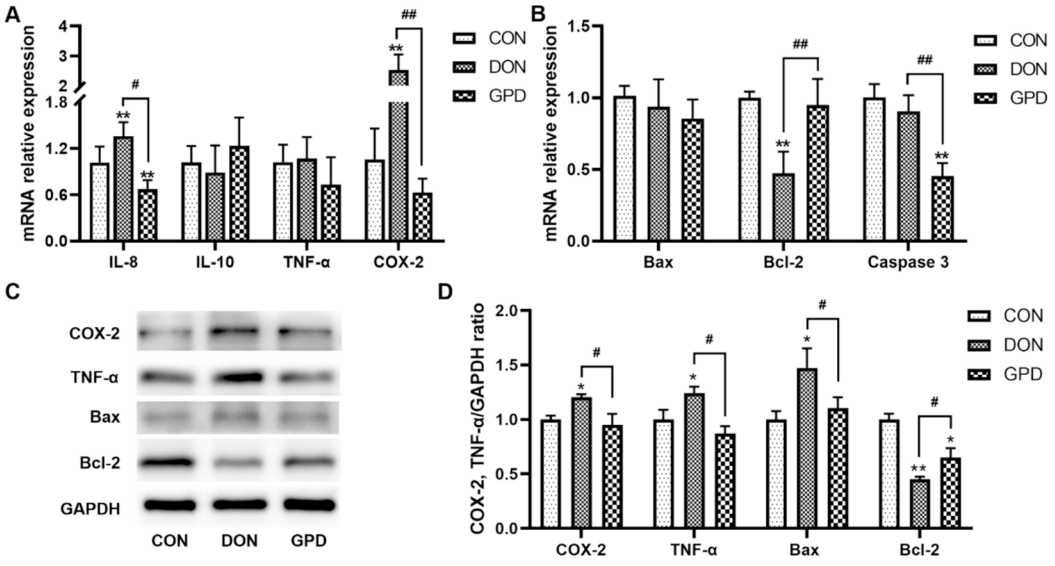

Fig. 2. GAP alleviated liver inflammation and apoptosis in DON-contaminated piglets. (A-B) The mRNA relative expressions of IL-8, IL-10, COX-2, TNF-α, Caspase 3, Bax and Bcl-2. (C-D) The protein expression and quantitative analysis of COX-2, TNF-α, Bax and Bcl-2. * indicates $P < 0.05$, ** indicates $P < 0.01$ relative to the CON group; # indicates $P < 0.05$, ## indicates $P < 0.01$ relative to the DON group.

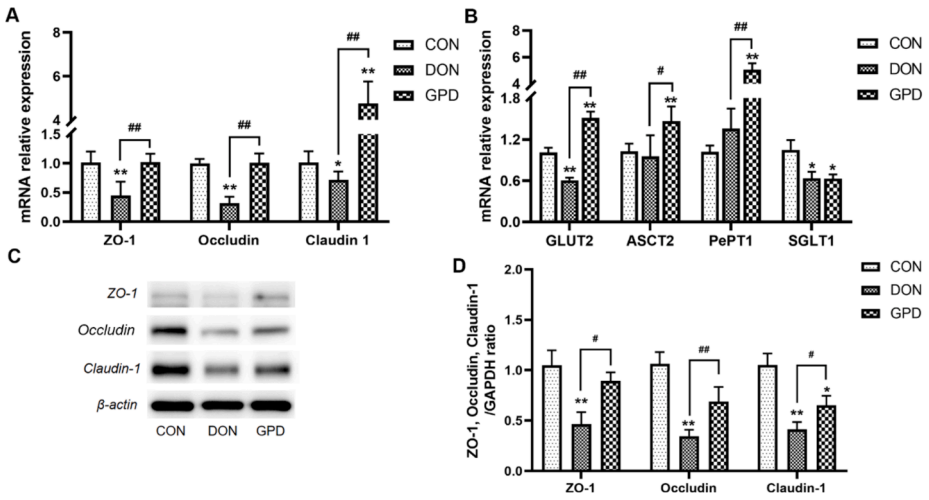

Fig. 3. GAP supplementation alleviated liver barrier function and nutrient transport in DON-contaminated piglets. (A-B) The mRNA relative expressions of ZO-1, Occludin, Claudin-1, GLUT2, ASCT2, PePT1 and SGLT1. (C-D) The protein expressions and quantitative analysis of ZO-1, Occludin and Claudin-1. * indicates $P < 0.05$, ** indicates $P < 0.01$ relative to the CON group; # indicates $P < 0.05$, ## indicates $P < 0.01$ relative to the DON group.

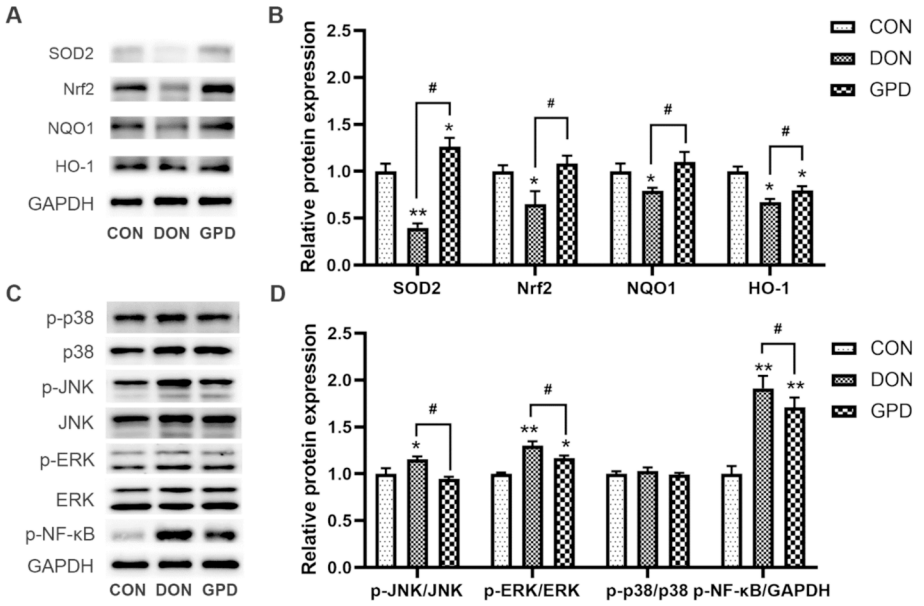

Fig. 4. Effects of GAP supplementation on Nrf2/MAPK/NF-κB pathways in liver of DON-contaminated piglets. (A-B) The protein expressions and quantification analysis for SOD2, Nrf2, NQO1 and HO-1. (C-D) The protein expressions and quantitative analysis of p-JNK, JNK, p-ERK, ERK, p-p38, p38 and p-NF-κB. * indicates $P < 0.05$, ** indicates $P < 0.01$ relative to the CON group; # indicates $P < 0.05$, ## indicates $P < 0.01$ relative to the DON group.

variance in phenotypic traits, respectively **(**Fig. 5**A)**. The PLS-DA model **(**Fig. 5**B)** demonstrated the model parameters ($R^2X = 0.723$, $R^2Y = 0.996$, $Q^2Y = 0.932$) for serum metabolites were all greater than 0.5, indicating a well-established and reliable model with strong predictive capabilities. Significant differences among the three groups were also observed, suggesting that serum metabolic characteristics were significantly influenced by DON exposure and GAP supplementation.

The differentially expressed metabolites analysis revealed that 201, 423 and 271 different metabolites were identified in CON vs. DON group, CON vs. GPD group and DON vs. GPD group, respectively. The volcano plot was utilized to identify the most significantly different metabolites in the treatment groups **(**Fig. 5**C)**. Compared to the CON group, the DON group displayed a increase in 77 metabolites and a decrease in 124 metabolites, while the GPD group exhibited a increase in 124 metabolites and a decrease in 299 metabolites. The GPD group showed a notable increase in 100 metabolites and a decrease in 171 metabolites compared to the DON group.

Venn diagram analysis of different metabolites in CON vs. DON, CON vs. GPD and DON vs. GPD groups revealed a total of 40 common different metabolites **(**Fig. 5**D)**. Among these, 34 differential metabolites were shared between the CON vs. DON group and DON vs. GPD group. Specifically, 18 metabolites were significantly downregulated in the CON vs. DON while significantly upregulated in the DON vs. GPD. Similarly, 19 metabolites were significantly upregulated in the CON vs. DON while significantly downregulated in the DON vs. GPD. The specific metabolites were detailed in Table 1 (the first 34 are the common differential metabolites among the three groups).

To enhance the visualization of changes in metabolite abundance among the treatment groups, a heatmap clustering analysis was performed on the 34 common different metabolites in the nine samples **(**Fig. 5**E)**. Specifically, the GPD group had a significant increase in the levels of metabolites including PC (18:1(11Z)/22:5(7Z, 10Z, 13Z, 16Z,

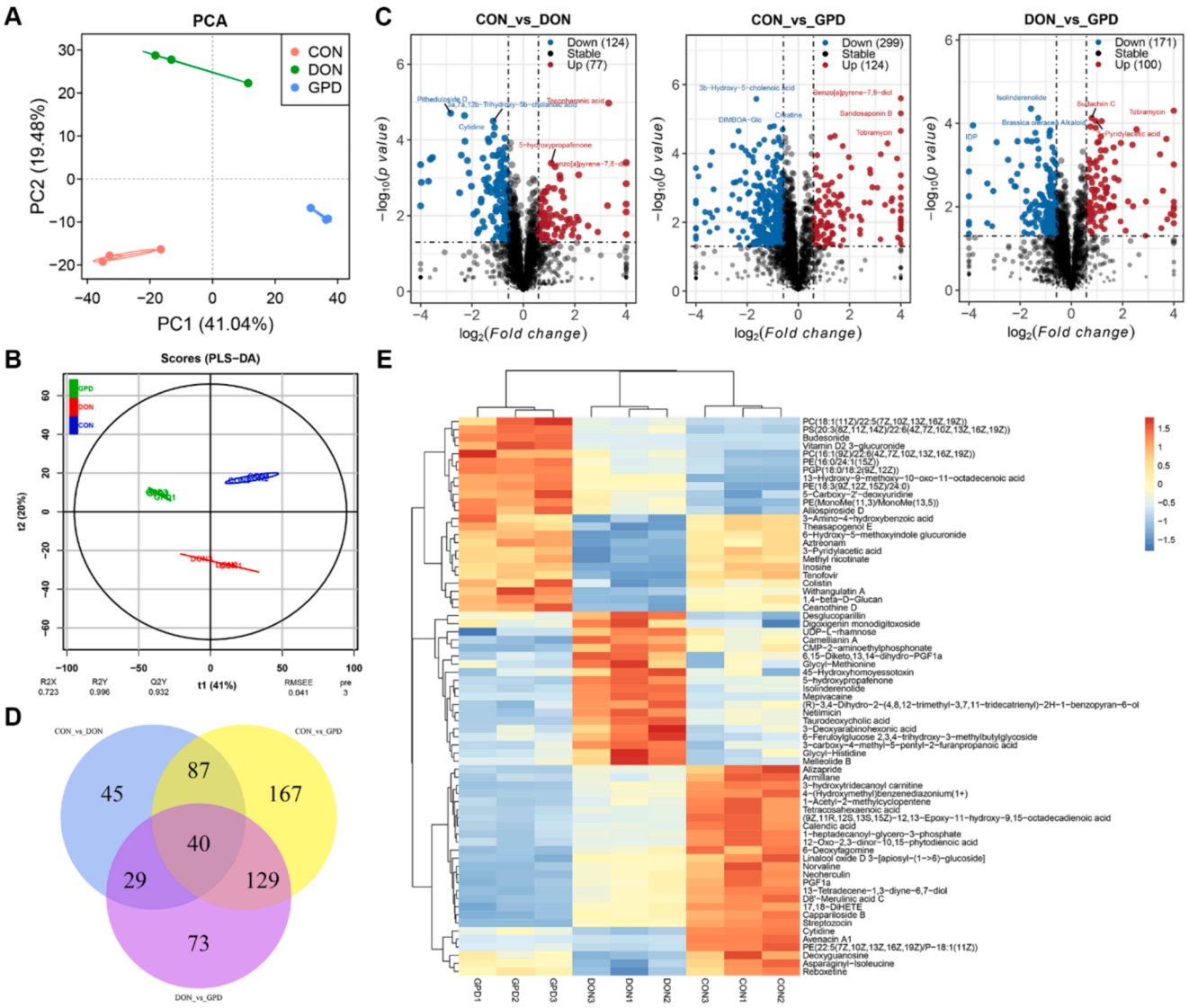

Fig. 5. Analysis of serum metabolites in weaned piglets. (A) PCA analysis. (B) PLS-DA model analysis. (C) Volcanic map of differences in metabolites among different groups. (D) Venn map of differential metabolites in CON vs. DON group, CON vs. GPD group and DON vs. GPD group, respectively. (E) Heat map of the total of 34 differential metabolites in different groups.

19Z)), PE (16:0/24:1(15Z)), vitamin D2 3-glucuronide, colistin, theasapogenol E, 3-amino-4-hydroxybenzoic acid, asparaginyl-Isoleucine, deoxyguanosine, 1,4-β-D-glucan, methyl nicotinate, 3-pyridylacetic acid, inosine and some glycerophospholipids ($P < 0.05$) compared with the DON group. Conversely, it markedly reduced the levels of metabolites such as 3-deoxyarabinohexonic acid, isolinderenolide, desglucoparillin, glycyl-histidine, and taurodeoxycholic acid ($P < 0.05$).

3.6. KEGG enrichment analysis

To enhance comprehension on the impacts of differential metabolites among serum samples of weaned piglets, KEGG metabolic pathway enrichment was analyzed. As demonstrated in Fig. 6, DON primarily perturbed metabolic pathways such as α-linolenic acid metabolism, linoleic acid metabolism, terpenoid backbone biosynthesis, chemical carcinogenesis, and phosphonate and phosphinate metabolism. At the same time, glufosinate was found to affect pathways including glycerophospholipid metabolism, retrograde endocannabinoid signaling, α-linolenic acid metabolism, arachidonic acid metabolism, and linoleic acid metabolism. Additionally, compared with the DON group, GPD impact extended to metabolic pathways distinct from DON, such as α-linolenic acid metabolism, purine metabolism, carbon metabolism, glutathione metabolism, linolenic acid metabolism, steroid hormone biosynthesis. KEGG enrichment analysis was further performed for 34 different metabolites in CON vs. DON and DON vs. GPD groups, which were primarily concentrated in carbohydrate digestion and absorption, α-linolenic acid metabolism, linoleic acid metabolism and glycerophospholipid metabolism. These findings underscore the predominant effects of GPD on pathways involving glycerophospholipids, linoleic acid, α-linolenic acid, amino sugars, and nucleotide sugars, as well as starch and sucrose metabolism. GPD appears to mitigate the detrimental effects induced by DON through these targeted metabolic interventions.

3.7. Correlation analysis

In our previous study, we quantified the contents of AST and ALT in the serum, as well as the DON residues in the serum and feces of weaned piglets (Xu et al., 2023). As illustrated in Fig. 7**A**, correlation analysis was conducted to investigate the interplay between oxidative stress-related indices, inflammatory factors and DON residues within the serum and liver of these piglets. ALT levels in the serum of piglets were found to be significantly correlated with oxidative stress-related indices

Table 1
The expression levels of co-expressed differential metabolites in different samples.

Differential metabolites name	CON	DON	GPD	CON vs. DON	DON vs. GPD
1-Acetyl-2-methylcyclopentene	8.71E-06	4.38E-06	2.82E-06	down	down
(9Z,11R,12S,13S,15Z)-12,13-Epoxy-11-hydroxy-9,15-octadecadienoic acid	1.92E-05	7.13E-06	4.61E-06	down	down
1-heptadecanoyl-*glycero*-3-phosphate	3.96E-05	1.90E-05	1.21E-05	down	down
12-Oxo-2,3-dinor-10,15-phytodienoic acid	9.69E-06	3.65E-06	2.08E-06	down	down
13-Hydroxy-9-methoxy-10-oxo-11-octadecenoic acid	2.64E-05	1.17E-04	1.96E-04	up	up
13-Tetradecene-1,3-diyne-6,7-diol	1.14E-04	7.13E-05	3.75E-05	down	down
17,18-DiHETE	1.16E-05	7.36E-06	3.02E-06	down	down
3-hydroxytridecanoyl carnitine	8.95E-04	4.87E-04	2.60E-04	down	down
4-(Hydroxymethyl) benzenediazonium (1 +)	1.46E-05	7.12E-06	3.76E-06	down	down
5-Carboxy-2′-deoxyuridine	2.68E-06	5.11E-06	8.67E-06	up	up
6-Deoxyfagomine	1.11E-05	6.24E-06	2.69E-06	down	down
Alizapride	1.04E-05	3.02E-06	1.91E-07	down	down
Armillane	1.12E-05	3.59E-06	1.75E-06	down	down
Avenacin A1	2.04E-04	5.19E-06	1.36E-05	down	up
Calendic acid	1.17E-05	4.56E-06	2.82E-06	down	down
Cappariloside B	1.27E-05	8.07E-06	3.05E-06	down	down
Cytidine	1.27E-05	2.59E-06	5.61E-06	down	up
D8′-Merulinic acid C	7.46E-05	4.71E-05	2.68E-05	down	down
Deoxyguanosine	7.81E-06	2.05E-06	4.93E-06	down	up
Linalool oxide D 3-[apiosyl-(1->6)-glucoside]	5.64E-06	3.05E-06	5.51E-07	down	down
Neoherculin	5.95E-05	3.79E-05	1.81E-05	down	down
Netilmicin	6.77E-06	1.80E-05	2.39E-06	up	down
Norvaline	4.14E-05	2.66E-05	1.47E-05	down	down
PC(16:1(9Z)/22:6(4Z,7Z,10Z,13Z,16Z,19Z))	1.71E-03	1.27E-02	3.20E-02	up	up
PC(18:1(11Z)/22:5(7Z,10Z,13Z,16Z,19Z))	2.48E-04	8.41E-04	3.65E-03	up	up
PE(16:0/24:1(15Z))	2.26E-04	1.00E-03	3.28E-03	up	up
PE(18:3(9Z,12Z,15Z)/24:0)	3.80E-04	1.41E-03	2.65E-03	up	up
PE(22:5(7Z,10Z,13Z,16Z,19Z)/P-18:1(11Z))	9.28E-05	1.74E-05	2.75E-05	down	up
PE(MonoMe(11,3)/MonoMe(13,5))	1.89E-04	1.08E-03	2.11E-03	up	up
PGF1a	4.59E-05	2.98E-05	1.65E-05	down	down
PGP(18:0/18:2(9Z,12Z))	2.64E-04	1.17E-03	3.26E-03	up	up
PS(20:3(8Z,11Z,14Z)/22:6(4Z,7Z,10Z,13Z,16Z,19Z))	2.83E-05	4.98E-05	1.11E-04	up	up
Streptozocin	4.86E-05	2.80E-05	8.45E-06	down	down
Tetracosahexaenoic acid	2.02E-05	8.46E-06	5.38E-06	down	down
(R)-3,4-Dihydro-2-(4,8,12-trimethyl-3,7,11-tridecatrienyl)–2H-1-benzopyran-6-ol	6.79E-06	1.22E-05	4.91E-06	up	down
1,4-beta-D-Glucan	7.09E-05	2.03E-05	1.06E-04	down	up
3-Amino-4-hydroxybenzoic acid	1.61E-06	1.24E-07	1.82E-06	down	up
3-carboxy-4-methyl-5-pentyl-2-furanpropanoic acid	2.42E-05	4.15E-05	2.38E-05	up	down
3-Deoxyarabinohexonic acid	5.18E-06	9.33E-06	4.99E-06	up	down
3-Pyridylacetic acid	7.27E-04	3.86E-04	7.45E-04	down	up
45-Hydroxyhomoyessotoxin	1.57E-05	3.79E-05	1.42E-05	up	down
5-hydroxypropafenone	1.05E-05	2.23E-05	7.62E-06	up	down
6-Feruloylglucose 2,3,4-trihydroxy-3-methylbutylglycoside	1.05E-04	1.68E-04	1.12E-04	up	down
6-Hydroxy-5-methoxyindole glucuronide	1.48E-04	7.35E-05	1.67E-04	down	up
6,15-Diketo,13,14-dihydro-PGF1a	5.69E-06	1.09E-05	5.01E-06	up	down
Alliospiroside D	3.80E-07	1.46E-06	3.22E-06	up	up
Asparaginyl-Isoleucine	6.58E-05	3.27E-05	5.03E-05	down	up
Aztreonam	1.02E-05	4.89E-06	1.22E-05	down	up
Budesonide	0	5.06E-06	6.62E-05	up	up
Camellianin A	2.08E-05	3.64E-05	8.46E-06	up	down
Ceanothine D	1.71E-04	1.03E-04	2.32E-04	down	up
CMP-2-aminoethylphosphonate	2.81E-06	5.42E-06	1.06E-07	up	down
Colistin	8.67E-06	4.81E-06	1.16E-05	down	up
Desglucoparillin	2.34E-04	4.61E-04	3.07E-04	up	down
Digoxigenin monodigitoxoside	4.19E-06	1.64E-05	8.52E-06	up	down
Glycyl-Histidine	1.12E-05	1.93E-05	1.13E-05	up	down
Glycyl-Methionine	1.82E-06	6.34E-06	2.03E-06	up	down
Inosine	5.87E-05	2.47E-05	6.02E-05	down	up
Isolinderenolide	6.20E-06	1.46E-05	4.88E-06	up	down
Melleolide B	1.02E-04	1.80E-04	1.14E-04	up	down
Mepivacaine	0	2.75E-05	0.00E + 00	up	down
Methyl nicotinate	1.38E-03	7.29E-04	1.47E-03	down	up
Reboxetine	6.14E-06	2.87E-06	4.97E-06	down	up
Taurodeoxycholic acid	5.86E-04	9.83E-04	4.40E-04	up	down
Tenofovir	4.15E-05	2.44E-05	4.09E-05	down	up
Theasapogenol E	1.71E-05	9.92E-06	1.84E-05	down	up
UDP-L-rhamnose	2.53E-06	3.94E-06	1.35E-06	up	down
Vitamin D2,3-glucuronide	6.49E-06	1.94E-05	1.03E-04	up	up
Withangulatin A	3.61E-06	1.96E-06	6.11E-06	down	up

Note: The first 34 metabolites exist in CON vs. DON and DON vs. GPD group. E stands for scientific enumeration, which is 10 to the minus some power.

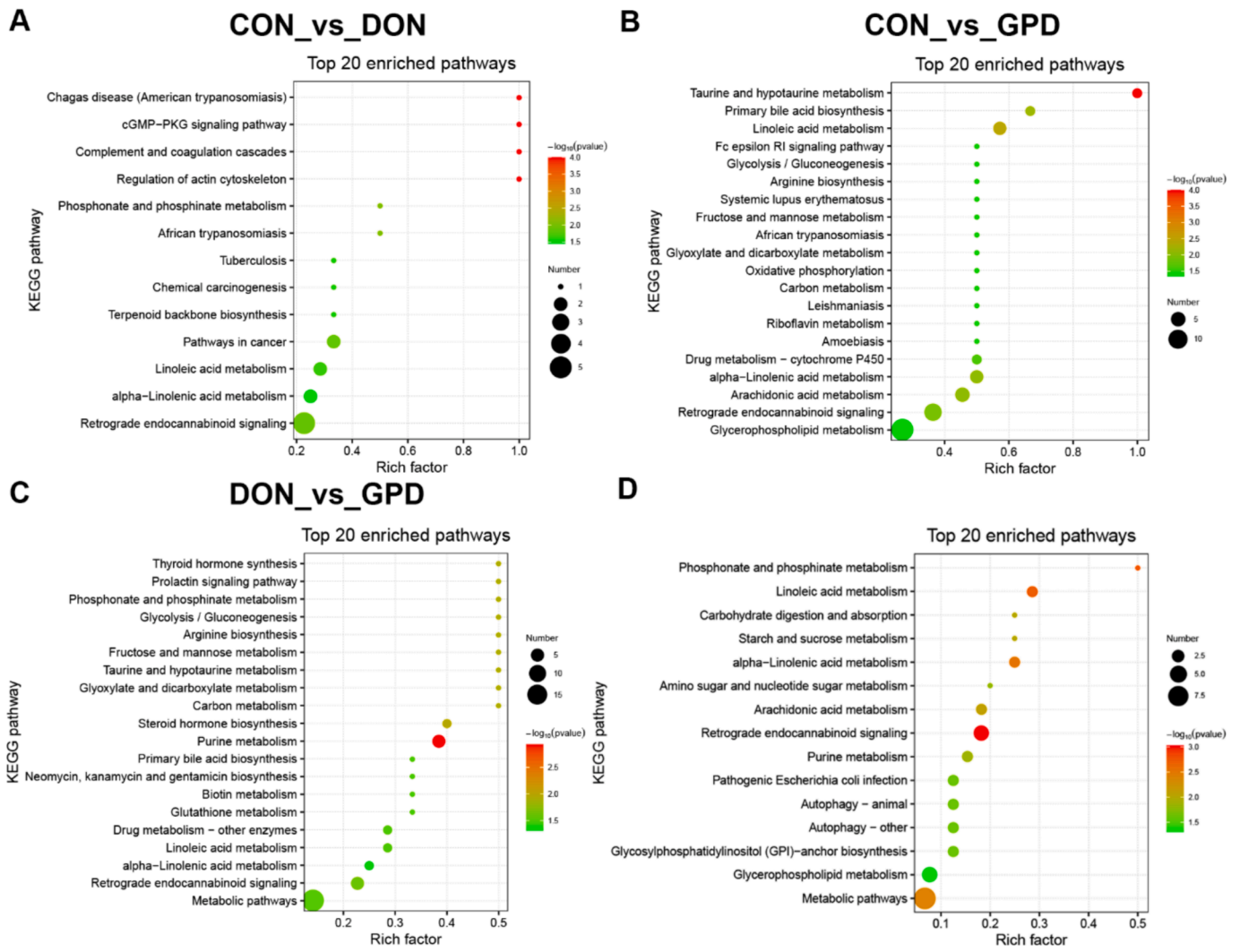

Fig. 6. Analysis of enriched KEGG pathways for differential metabolites in serum of weaned piglets. (A-C) The top 20 enriched pathways of different metabolites. (D) A total of 34 different metabolites were enriched in KEGG pathways between the CON vs. DON group and DON vs. GPD group.

in the serum and liver (SOD and CAT), as well as with DON residues and the inflammatory factor NF-κB. Additionally, oxidative stress-related indices in serum were strongly correlated with inflammatory factors (IL-8, NF-κB) and DON residues, as well as with oxidative stress-related indices (MDA, SOD, CAT, GSH-Px) in liver. Furthermore, serum inflammatory factors were found to be significantly correlated with oxidative stress-related indicesin liver. Moreover, the results also demonstrated a substantial correlation between DON residues and oxidative stress indicators in the liver, including SOD, CAT, GSH-Px and MDA. These correlation analyses suggested that the modulation of oxidative stress and inflammatory responses is crucial in mitigating the DON-induced liver injury in piglets. Fig. 7**B** exhibited the correlation between differential metabolites in the serum and oxidative stress-related indicators, inflammatory factors and residues of DON in serum and liver. The metabolites 5-carboxy-2′-deoxyuridine, budesonide, vitamin D2 3-glucuronide, PE (monome(11,3)/monome(13,5)), alliospiroside D, PE (18:3(9Z, 12Z, 15Z)/24:0), PGP (18:0/18:2(9Z,12Z)) and PE (16:0/24:1(15Z)) were significantly negatively correlated with antioxidant indices (SOD, CAT and GSH-Px) in piglet livers ($P < 0.05$). In contrast, a significant positive correlation was observed between these metabolites and DON residues in the liver ($P < 0.05$). The metabolites of 17,18-dihete, alizapride, armillane and tetracosahexaenoic acid were significantly positively correlated with antioxidant indices (SOD, CAT and GSH-Px) in the piglet livers ($P < 0.05$). Additionally, a significant negative correlation was observed between these metabolites and oxidative stress-related indices (MDA, LDH) ($P < 0.05$).

4. Discussion

The liver plays a crucial part in upholding general well-being and controlling illnesses in both humans and animals (Zhang et al., 2022). Therefore, reducing liver injury is a universally recognized and highly effective strategy for safeguarding human and animal health. DON, the dominant mycotoxin in human and animal food, predominantly accumulates in the liver following absorption by the body, leading to liver damage that includes inflammation (Li et al., 2022), oxidative stress (Meng et al., 2021) and lipid metabolism disorders (Zong et al., 2022). In this study, histological analysis of weaned piglets exposed to DON demonstrated severe inflammation, nuclear dissolution, and rupture. MDA is considered a critical indicator of oxidative stress (Mehrabani et al., 2023), and antioxidant enzymes are the primary defense against ROS (Li et al., 2022). Dietary DON contamination markedly increased the MDA content and decreased antioxidant enzymes in serum and liver, triggering oxidative stress in piglets (Ji et al., 2023). GA, the principal active constituent of licorice, is recognized as an effective treatment for liver diseases due to its ability to improve liver inflammation (Ming & Yin, 2013; Yuan et al., 2019). Furthermore, it has been suggested that the addition of probiotics can increase liver antioxidative capacity and

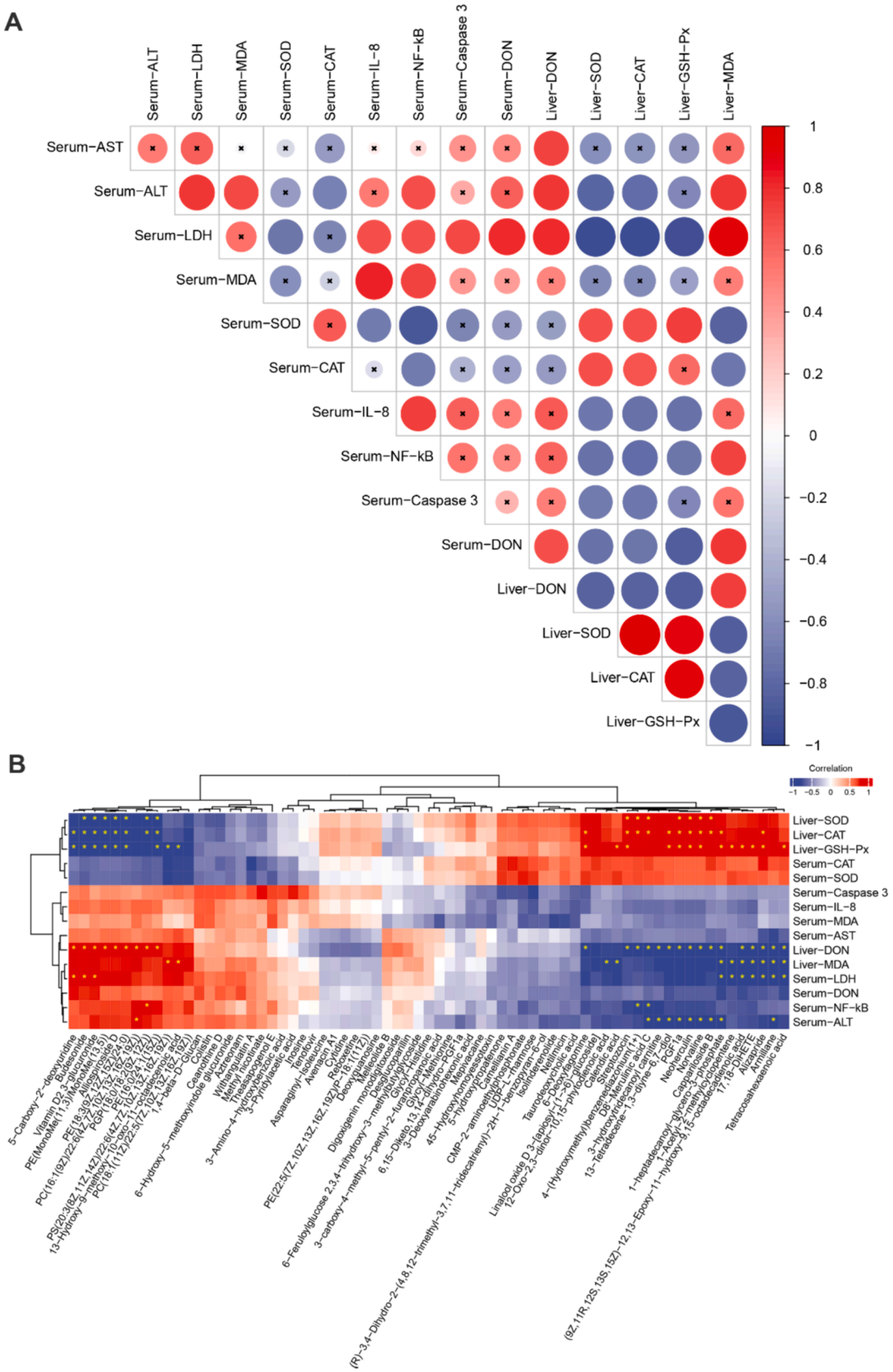

Fig. 7. Correlation analysis of differential metabolites with different indicators. (A) Correlation analysis of between oxidative stress-related indices, inflammatory factors and DON residues in the serum and liver of weaned piglets. "×" represents the correlation is not significant. (B) Correlation analysis of serum differential metabolites with oxidative stress-related indices, inflammatory factors and residues of DON in the serum and liver of weaned piglets.

decrease DON-induced oxidative stress (Bai et al., 2021). Interestingly, dietary supplementation of GAP alleviated DON-induced liver inflammation, increased antioxidant enzyme activity, and thereby enhanced the antioxidant capacity of piglet serum and liver in this study.

Inflammatory response is one of the mechanisms through which DON induces liver damage (Bai et al., 2021). Cytokines are essential to the processes of inflammation and immune response. DON induced the IL-6, IL-1β and TNF-α levels, activating inflammation and apoptosis (Chen et al., 2023). In this study, DON treatment significantly increased the levels of IL-8, COX-2, TNF-α, Bax and Caspase-3, while reduced the level of Bcl-2. Interestingly, after GAP supplementation, the damage was partially reversed, highlighting the efficacy of GAP in mitigating inflammation and apoptosis caused by DON. Furthermore, DON exposure markedly enhanced the serum concentrations of IL-8, Caspase 3, and NF-κB in piglets, whereas supplemented GAP decreased these indexes. In this study, the consistency of serum cytokine concentrations, cytokine mRNA abundance and protein expression in liver tissue confirmed that GAP could effectively counteract DON-induced inflammation and apoptosis.

Tight connections are essential to the preservation of the liver's structure and functionality. Cholestasis affects the expression of liver tight junction proteins (Maly & Landmann, 2008). ZO-1 expression was downregulated in diseased liver tissue (Zhang et al., 2019). Furthermore, research has indicated that alterations in intestinal barrier function can induce liver damage and metabolic disorders in the liver (Liu et al., 2023; Tilg et al., 2022). Previous work has demonstrated that the intake of DON can compromise the integrity of the intestinal barrier and interfere with the digestive and absorptive functions of the intestine (Xu et al., 2023). Therefore, this experiment examined the effect by DON pollution on the liver barrier function and transport of nutrients in piglets. Our results revealed that DON markedly reduced the levels of tight junction protein and nutrient transporter expression, resulting in impaired liver barrier function and nutrient absorption. However, GAP alleviated DON-linked liver barrier damage and maintained nutrient absorption and utilization rates.

DON exposure caused oxidative stress in the organism, triggering the activation of the Nrf2 protein, which translocated to the nucleus to bind with the antioxidant response element (ARE) and modulate the transcription of downstream antioxidant genes, including GSH, SOD, HO-1, and NQO1 (Chen et al., 2024). Previous study has reported that dihydroartemisinin could ameliorate the impact of DON on the antioxidant capacity of piglet livers, but the underlying mechanism was not thoroughly investigated (Li et al., 2022). Numerous studies have demonstrated that activity of the Nrf2 pathway alleviates DON-related oxidative stress (Yu et al., 2017; Zhu et al., 2023). This study indicated that GAP not only enhanced the activity of antioxidant enzymes (SOD and CAT) in the liver and serum but also activated Nrf2 pathway, leading to an upregulation of downstream antioxidant proteins (SOD2, NQO1, and HO-1). The MAPK signaling pathway, primarily involving ERK, JNK and p38, plays a pivotal role in cell proliferation, differentiation, inflammation, apoptosis and oxidative stress (Asl et al., 2021). DON can activate ERK, JNK and p38, thereby inducing inflammation and apoptosis through the MAPK signaling pathway (Lee et al., 2019). It is noteworthy that the MAPK plays a pivotal part in the orchestration downstream activity of NF-κB, resulting in the formation of different inflammatory mediators in liver injury (Li et al., 2021). The NF-κB pathway, a prototypical immune and inflammatory signaling pathway, significantly regulates the closely interconnected barrier (Al-Sadi et al., 2010). In this study, DON significantly elevated the content and protein expression levels of NF-κB. Interestingly, GAP administration significantly reduced the protein levels of DON-induced p-ERK, p-JNK, and NF-κB of the liver, with no impact on p-p38 in this study. This statement is inconsistent with previously published studies showing DON enhanced the p-p38 protein expression in the liver of mice (Hu et al., 2023), possibly due to differences in the origin and species of DON. Collectively, these results suggest that GAP mitigated DON-related liver damage through the activation of Nrf2-mediated antioxidant pathway and the inhibition of the MAPK/NF-κB-mediated inflammatory response and tight junction dysfunction pathway.

Drugs are metabolized in the liver before entering the bloodstream, therefore, the expression level of serum metabolites can be observed to assess the state of the liver (Ming et al., 2017). Furthermore, it was previously shown that dihydromyricetin could restore metabolic pathway disorders caused by DON, including glutamate metabolism, arachidonic acid metabolism, and histamine metabolism, thereby alleviating cell damage caused by DON (Long et al., 2021). In the present study, KEGG enrichment analysis revealed that these metabolites were predominantly associated with glycerophospholipid metabolism, linoleic acid metabolism, α-linolenic acid metabolism, and carbohydrate digestion and absorption pathways. These findings suggest that GAP could potentially mitigate DON-induced damage by regulating lipid metabolism in weaned piglets. It has been reported that the glycerophospholipid metabolism is the main metabolic pathway in which DON causes alterations in serum metabolites (Li et al., 2021). Notably, phosphatidylcholine (PC) and phosphatidylethanolamine (PE) have been identified as crucial metabolites within this pathway (Shi et al., 2022), which corroborates the findings of the present study. In the liver, PC is a fundamental constituent of the cell membrane. PE can regulate membrane fusions and provide ethanolamine. They play vital roles in signal transduction and phospholipid metabolism (Shi et al., 2022). Research has shown that in the event of liver injury, the concentrations of PC and PE were reduced (Ming et al., 2017), and reducing PE levels accelerates the ROS, leading to oxidative stress (Rockenfeller et al., 2015). The results revealed GAP administration markedly upregulated PC, PE, and PS metabolites compared to the DON group, indicating that GAP alleviated DON-caused oxidative stress through regulation of lipid metabolism.

Moreover, 5-carboxy-2′-deoxyuridine has been employed to monitor diseases associated with oxidative stress, metabolic abnormalities and environmental exposures. A study revealed that the concentration of 5-carboxy-2′-deoxyuridine in colorectal cancer tissues was lower than that in normal tissues (Gackowski et al., 2016). The results of this study indicated that 5-carboxy-2′-deoxyuridine exhibits a significant inverse correlation with antioxidant indices (SOD, CAT and GSH-Px) and a remarkable positive correlation with DON residues in the liver of piglets. This suggested that DON intake in piglets led to metabolic abnormalities and oxidative stress, thereby damaging the liver. Research reported that L-norvaline could reduce lipid peroxidation and prevent diabetes (Javrushyan et al., 2022). The reduction in norvaline levels increases the risk of liver disease (Liu et al., 2024). Norvaline showed a significant positive correlation with liver antioxidant enzymes (SOD, CAT, and GSH-Px) and a significant negative correlation with the residue of DON in the liver and the content of ALT in the serum, indicating that DON affected the expression of norvaline, leading to lipid peroxidation, which in turn caused liver damage. Armillane is a compound isolated from *Armillaria* species that inhibits fungal and tumor activity and modulates the body immunity (Li et al., 2023). Tetracosahexaenoic acid as the product and precursor of DHA in rodents, regulates lipid metabolism and is crucial for organism growth and development (Metherel & Bazinet, 2019; Metherel et al., 2019). Studies indicated that a defect in the synthesis of tetracosahexaenoic acid in the liver could lead to Alzheimer's disease (Astarita et al., 2010). This paper demonstrated a significant positive correlation between the metabolites armillane and tetracosahexaenoic acid and antioxidant indexes (SOD, CAT, and GSH-Px), as well as a significant negative correlation with DON residues and the levels of MDA and LDH. Overall, these results indicated that DON intake led to lipid metabolism disorders in weaned piglets, whereas GAP could improve lipid metabolism, thereby alleviating the toxicity of DON and promoting the healthy growth of piglets.

In our results, we indicated that supplementation of DON-containing diets with GAP markedly mitigated the hepatotoxic effect of DON in piglets. The underlying mechanisms involved appear to be that GAP

prevents the liver damage caused by DON-induced damage via enhancing lipid metabolism, thereby reducing oxidative stress, inflammation and apoptosis in the liver, increasing liver barrier function and nutrient transport, and regulating Nrf2/MAPK/NF-κB pathway. Furthermore, our research was specifically focused on the protection provided by GAP on the liver of piglets in vivo. In future studies, we will explore the long-term effects of different dosages or durations of GAP supplementation on the organism, and expect to translate the findings into clinical applications.

5. Conclusions

In this investigation, GAP supplemented to DON-polluted diet safeguarded the liver of weaned piglets from DON-induced damage by regulating lipid metabolism, enhancing antioxidant and anti-inflammatory capacity, improving the stability of liver barrier structure and nutrient transport function, and modulating the Nrf2/MAPK/NF-κB pathway. Overall, our study provides new evidence to support the efficacy of compound probiotics and GA administration in ameliorating DON-induced liver damage in humans and animals.

Ethics Statement

The animal experimental protocols in this research adhered to the Chinese Guidelines for Institutional Animal Welfare and were authorized by the Animal Care and Use Committee of Henan Agricultural University (SKLAB-B-2010–003–01).

CRediT authorship contribution statement

Mengjie Liu: Writing – original draft, Methodology, Investigation, Data curation. **Guorong Yan:** Visualization, Formal analysis, Data curation. **Juan Chang:** Resources, Project administration, Methodology, Investigation. **Ping Wang:** Methodology, Investigation. **Chaoqi Liu:** Validation, Methodology, Investigation. **Qingqiang Yin:** Writing – review & editing, Supervision, Methodology, Investigation. **Xiaoxiang Xu:** Writing – review & editing, Project administration, Methodology, Investigation, Funding acquisition.

Declaration of competing interest

The authors declare that they have no known competing financial interests or personal relationships that could have appeared to influence the work reported in this paper.

Data availability

Data will be made available on request.

Acknowledgments

Funding for this study was provided by the National Natural Science Foundation of China (82203942), the Xinxiang Key Scientific and Technological Projects (22ZD011) and the Postgraduate Education Reform and Quality Improvement Project of Henan Province (YJS2023JD18).

References

Al-Sadi, R., Ye, D., Said, H. M., & Ma, T. Y. (2010). IL-1β-induced increase in intestinal epithelial tight junction permeability is mediated by MEKK-1 activation of canonical NF-κB pathway. *The American Journal of Pathology, 177*(5), 2310–2322. https://doi.org/10.2353/ajpath.2010.100371

Asl, E. R., Amini, M., Najafi, S., Mansoori, B., Mokhtarzadeh, A., Mohammadi, A., Lotfinejad, P., Bagheri, M., Shirjang, S., Lotfi, Z., Rasmi, Y., & Baradaran, B. (2021). Interplay between MAPK/ERK signaling pathway and MicroRNAs: A crucial mechanism regulating cancer cell metabolism and tumor progression. *Life Sciences, 278*, Article 119499. https://doi.org/10.1016/j.lfs.2021.119499

Astarita, G., Jung, K. M., Berchtold, N. C., Nguyen, V. Q., Gillen, D. L., Head, E., Cotman, C. W., & Piomelli, D. (2010). Deficient liver biosynthesis of docosahexaenoic acid correlates with cognitive impairment in Alzheimer's disease. *PLoS One, 5*(9), e12538. https://doi.org/10.1371/journal.pone.0012538

Bai, Y. S., Ma, K. D., Li, J. B., Li, J. P., Bi, C. P., & Shan, A. S. (2021). Deoxynivalenol exposure induces liver damage in mice: Inflammation and immune responses, oxidative stress, and protective effects of *Lactobacillus rhamnosus* GG. *Food and Chemical Toxicology, 156*, Article 112514. https://doi.org/10.1016/j.fct.2021.112514

Chen, H., Chen, X., & Ma, J. (2023). The mitigation mechanism of hesperidin on deoxynivalenol toxicity in grass carp hepatocytes via decreasing ROS accumulation and inhibiting JNK phosphorylation. *Fish & Shellfish Immunology, 134*, Article 108646. https://doi.org/10.1016/j.fsi.2023.108646

Chen, J. S., Zhou, Z. Y., Wu, N. H., Li, J., Xi, N. Y., Xu, M. Y., Wu, F., Fu, Q. T., Yan, G. R., Liu, Y. Q., & Xu, X. X. (2024). Chlorogenic acid attenuates deoxynivalenol-induced apoptosis and pyroptosis in human keratinocytes via activating Nrf2/HO-1 and inhibiting MAPK/NF-κB/NLRP3 pathways. *Biomedicine & Pharmacotherapy, 170*, Article 116003. https://doi.org/10.1016/j.biopha.2023.116003

Chen, Y., Wang, H., Zhai, N., Wang, C., Huang, K., & Pan, C. (2019). Nontoxic concentrations of OTA aggravate DON-induced intestinal barrier dysfunction in IPEC-J2 cells via activation of NF-κB signaling pathway. *Toxicology Letters, 311*, 114–124. https://doi.org/10.1016/j.toxlet.2019.04.021

de Souza, M., Baptista, A. A. S., Valdiviezo, M. J. J., Justino, L., Menck-Costa, M. F., Ferraz, C. R., da Gloria, E. M., Verri, W. A., & Bracarense, A. P. F. R. L. (2020). *Lactobacillus* spp. reduces morphological changes and oxidative stress induced by deoxynivalenol on the intestine and liver of broilers. *Toxicon, 185*, 203–212. https://doi.org/10.1016/j.toxicon.2020.07.002

Feng, N. N., Zhong, F., Cai, G. D., Zheng, W. L., Zou, H., Gu, J. H., Yuan, Y., Zhu, G. Q., Liu, Z. P., & Bian, J. C. (2023). *Fusarium* mycotoxins zearalenone and deoxynivalenol reduce hepatocyte innate immune response after the *Listeria monocytogenes* infection by inhibiting the TLR2/NF-κB signaling pathway. *International Journal of Molecular Sciences, 24*(11), 9664. https://doi.org/10.3390/ijms24119664

Gackowski, D., Starczak, M., Zarakowska, E., Modrzejewska, M., Szpila, A., Banaszkiewicz, Z., & Olinski, R. (2016). Accurate, direct, and high-throughput analyses of a broad spectrum of endogenously generated DNA base modifications with isotope-dilution two-dimensional ultraperformance liquid chromatography with tandem mass spectrometry: Possible clinical implication. *Analytical Chemistry, 88*(24), 12128–12136. https://doi.org/10.1021/acs.analchem.6b02900

Hasuda, A. L., Person, E., Khoshal, A. K., Bruel, S., Puel, S., Oswald, I. P., Bracarense, A. P. F. R. L., & Pinton, P. (2022). Deoxynivalenol induces apoptosis and inflammation in the liver: Analysis using precision-cut liver slices. *Food and Chemical Toxicology, 163*, Article 112930. https://doi.org/10.1016/j.fct.2022.112930

Hu, P., Liu, Y. Y., Li, S. C., Zhao, Y. H., Gu, H. T., Zong, Q. F., Ahmed, A. A., Bao, W. B., Liu, H. Y., & Cai, D. M. (2023). Lactoferrin Relieves Deoxynivalenol-induced oxidative stress and inflammatory response by modulating the Nrf2/MAPK pathways in the liver. *Journal of Agricultural and Food Chemistry, 71*(21), 8182–8191. https://doi.org/10.1021/acs.jafc.3c01035

Javrushyan, H., Nadiryan, E., Grigoryan, A., Avtandilyan, N., & Maloyan, A. (2022). Antihyperglycemic activity of L-norvaline and L-arginine in high-fat diet and streptozotocin-treated male rats. *Experimental and Molecular Pathology, 126*, Article 104763. https://doi.org/10.1016/j.yexmp.2022.104763

Ji, X., Tang, Z. Q., Zhang, F., Zhou, F., Wu, Y. J., & Wu, D. (2023). Dietary taurine supplementation counteracts deoxynivalenol-induced liver injury via alleviating oxidative stress, mitochondrial dysfunction, apoptosis, and inflammation in piglets. *Ecotoxicology and Environmental Safety, 253*, Article 114705. https://doi.org/10.1016/j.ecoenv.2023.114705

Jia, H., Liu, N., Zhang, Y. C., Wang, C., Yang, Y., & Wu, Z. L. (2021). 3-Acetyldeoxynivalenol induces cell death through endoplasmic reticulum stress in mouse liver. *Environmental Pollution, 286*, Article 117238. https://doi.org/10.1016/j.envpol.2021.117238

Lee, J. Y., Lim, W., Park, S., Kim, J., You, S., & Song, G. (2019). Deoxynivalenol induces apoptosis and disrupts cellular homeostasis through MAPK signaling pathways in bovine mammary epithelial cells. *Environmental Pollution, 252*, 879–887. https://doi.org/10.1016/j.envpol.2019.06.001

Li, F. C., Huang, L. B., Liu, Q. C., Wang, P. W., Chen, H. J., & Wang, C. Y. (2021). Different metabolites induced by deoxynivalenol in the serum and urine of weaned rabbits detected using LC-MS-based metabolomics. *Comparative Biochemistry and Physiology Part C: Toxicology & Pharmacology, 250*, Article 109184. https://doi.org/10.1016/j.cbpc.2021.109184

Li, J. B., Bai, Y. S., Ma, K. D., Ren, Z. S., Li, J. P., Zhang, J., & Shan, A. S. (2022). Dihydroartemisinin alleviates deoxynivalenol induced liver apoptosis and inflammation in piglets. *Ecotoxicology and Environmental Safety, 241*, Article 113811. https://doi.org/10.1016/j.ecoenv.2022.113811

Li, Y., Lou, S., Yang, R., Zhang, L., Zou, Q., Shang, S., Gao, L., & Wang, W. (2023). Cytotoxic sesquiterpene aryl esters from *Armillaria gallica* 012m. *Chinese Herbal Medicines, 15*(2), 343–346. https://doi.org/10.1016/j.chmed.2022.10.003

Li, Z. L., Zhao, Q. W., Lu, Y. J., Zhang, Y. X., Li, L. Y., Li, M., Chen, X. M., Sun, D. L., Duan, Y. F., & Xu, Y. (2021). DDIT4 s-nitrosylation aids p38-MAPK signaling complex assembly to promote hepatic reactive oxygen species production. *Advanced Science, 8*(18), 2101957. https://doi.org/10.1002/advs.202101957

Liu, C., Zhu, Y. H., Lu, Z. X., Guo, W. N., Tumen, B., He, Y. L., Chen, C., Hu, S. S., Xu, K. Z., Wang, Y., Li, L., & Li, S. H. (2020). Cadmium induces acute liver injury by inhibiting Nrf2 and the role of NF-κB, NLRP3, and MAPKs signaling pathway. *International Journal of Environmental Research and Public Health, 17*(1), 138. https://doi.org/10.3390/ijerph17010138

Liu, L., Yin, M. Y., Gao, J. W., Yu, C. Y., Lin, J. X., Wu, A. R., Zhu, J. Z., Xu, C. F., & Liu, X. L. (2023). Intestinal barrier function in the pathogenesis of nonalcoholic fatty liver disease. *Journal of Clinical and Translational Hepatology, 11*(2), 452–458. https://doi.org/10.14218/Jcth.2022.00089

Liu, M., Liu, C., Shi, J., Wang, P., Chang, J., Xu, X., Wang, L., Jin, S., Li, X., Yin, Q., Zhu, Q., Dang, X., & Lu, F. (2024). Corn straw-saccharification fiber improved the reproductive performance of sows in the late gestation and lactation via lipid metabolism. *Frontiers in Nutrition, 11*, 1370975. https://doi.org/10.3389/fnut.2024.1370975

Liu, Y., Yu, G., Medsker, H., Luo, T., Meng, X., Wang, C., Feng, L., & Zhang, J. (2024). Perinatal exposure to perfluorooctane sulfonate and the risk of hepatic inflammation in rat offspring: Perturbation of gut-liver crosstalk. *Environmental Research, 259*, Article 119442. https://doi.org/10.1016/j.envres.2024.119442

Long, H. R., Xin, Z. Q., Zhang, F., Zhai, Z. Y., Ni, X. J., Chen, J. L., Yang, K., Liao, P. F., Zhang, L. M., Xiao, Z. L., Sindaye, D., & Deng, B. C. (2021). The cytoprotective effects of dihydromyricetin and associated metabolic pathway changes on deoxynivalenol treated IPEC-J2 cells. *Food Chemistry, 338*, Article 128116. https://doi.org/10.1016/j.foodchem.2020.128116

Ma, R., Zhang, L., Liu, M., Su, Y. T., Xie, W. M., Zhang, N. Y., Dai, J. F., Wang, Y., Rajput, S. A., Qi, D. S., Karrow, N. A., & Sun, L. H. (2018). Individual and combined occurrence of mycotoxins in feed ingredients and complete feeds in China. *Toxins, 10*(3), 113. https://doi.org/10.3390/toxins10030113

Maly, I. P., & Landmann, L. (2008). Bile duct ligation in the rat causes upregulation of ZO-2 and decreased colocalization of claudins with ZO-1 and occludin. *Histochemistry and Cell Biology, 129*(3), 289–299. https://doi.org/10.1007/s00418-007-0374-7

Mao, X. X., Li, J., Xie, X., Chen, S., Huang, Q., Mu, P. Q., Jiang, J., & Deng, Y. Q. (2022). Deoxynivalenol induces caspase-3/GSDME-dependent pyroptosis and inflammation in mouse liver and HepaRG cells. *Archives of Toxicology, 96*(11), 3091–3112. https://doi.org/10.1007/s00204-022-03344-9

Maresca, M. (2013). From the gut to the brain: Journey and pathophysiological effects of the food-associated trichothecene mycotoxin deoxynivalenol. *Toxins, 5*(4), 784–820. https://doi.org/10.3390/toxins5040784

Mehrabani, S., Khorvash, F., Heidari, Z., Tajabadi-Ebrahimi, M., & Amani, R. (2023). The effects of synbiotic supplementation on oxidative stress markers, mental status, and quality of life in patients with Parkinson's disease: A double-blind, placebo-controlled, randomized controlled trial. *Journal of Functional Foods, 100*, Article 105397. https://doi.org/10.1016/j.jff.2022.105397

Meng, Z. T., Wang, L. L., Liao, Y. X., Peng, Z., Li, D., Zhou, X. L., Liu, S., Li, Y. M., Nuessler, A. K., Liu, L. G., Hao, L. P., & Yang, W. (2021). The protective effect of heme oxygenase-1 on liver injury caused by DON-induced oxidative stress and cytotoxicity. *Toxins, 13*(10), 732. https://doi.org/10.3390/toxins13100732

Metherel, A. H., & Bazinet, R. P. (2019). Updates to the n-3 polyunsaturated fatty acid biosynthesis pathway: DHA synthesis rates, tetracosahexaenoic acid and (minimal) retroconversion. *Progress in Lipid Research, 76*, Article 101008. https://doi.org/10.1016/j.plipres.2019.101008

Metherel, A. H., Lacombe, R. J. S., Chouinard-Watkins, R., & Bazinet, R. P. (2019). Docosahexaenoic acid is both a product of and a precursor to tetracosahexaenoic acid in the rat. *Journal of Lipid Research, 60*(2), 412–420. https://doi.org/10.1194/jlr.M090373

Ming, L. J., & Yin, A. C. Y. (2013). Therapeutic effects of glycyrrhizic acid. *Natural Product Communications, 8*(3), 415–418. https://doi.org/10.1177/1934578X1300800335

Ming, Y. N., Zhang, J. Y., Wang, X. L., Li, C. M., Ma, S. C., Wang, Z. Y., Liu, X. L., Li, X. B., & Mao, Y. M. (2017). Liquid chromatography mass spectrometry-based profiling of phosphatidylcholine and phosphatidylethanolamine in the plasma and liver of acetaminophen-induced liver injured mice. *Lipids in Health and Disease, 16*(1), 153. https://doi.org/10.1186/s12944-017-0540-4

Panisson, J. C., Wellington, M. O., Bosompem, M. A., Nagl, V., Schwartz-Zimmermann, H. E., & Columbus, D. A. (2023). Urinary and serum concentration of deoxynivalenol (DON) and DON metabolites as an indicator of DON contamination in swine diets. *Toxins, 15*(2), 120. https://doi.org/10.3390/toxins15020120

Rockenfeller, P., Koska, M., Pietrocola, F., Minois, N., Knittelfelder, O., Sica, V., Franz, J., Carmona-Gutierrez, D., Kroemer, G., & Madeo, F. (2015). Phosphatidylethanolamine positively regulates autophagy and longevity. *Cell Death and Differentiation, 22*(3), 499–508. https://doi.org/10.1038/cdd.2014.219

Saia, S., Fragasso, M., De Vita, P., & Beleggia, R. (2019). Metabolomics provides valuable insight for the study of durum wheat: A Review. *Journal of Agricultural and Food Chemistry, 67*(11), 3069–3085. https://doi.org/10.1021/acs.jafc.8b07097

Shi, Q. L., Wang, Q. X., Chen, J. Y., Xia, F., Qiu, C., Li, M., Zhao, M. H., Zhang, Q., Luo, P., Lu, T. M., Zhang, Y., Xu, L. T., He, X. L., Zhong, T. Y., Lin, N., & Guo, Q. Y. (2022). Transcriptome and lipid metabolomics-based discovery: Glycyrrhizic acid alleviates *Tripterygium* glycoside tablet-induced acute liver injury by regulating the activities of CYP and the metabolism of phosphoglycerides. *Frontiers in Pharmacology, 12*, Article 822154. https://doi.org/10.3389/fphar.2021.822154

Tang, M., Yuan, D. X., & Liao, P. (2021). Berberine improves intestinal barrier function and reduces inflammation, immunosuppression, and oxidative stress by regulating the NF-κB/MAPK signaling pathway in deoxynivalenol-challenged piglets. *Environmental Pollution, 289*, Article 117865. https://doi.org/10.1016/j.envpol.2021.117865

Tibola, C. S., Fernandes, J. M. C., & Guarienti, E. M. (2016). Effect of cleaning, sorting and milling processes in wheat mycotoxin content. *Food Control, 60*, 174–179. https://doi.org/10.1016/j.foodcont.2015.07.031

Tilg, H., Adolph, T. E., & Trauner, M. (2022). Gut-liver axis: Pathophysiological concepts and clinical implications. *Cell Metabolism, 34*(11), 1700–1718. https://doi.org/10.1016/j.cmet.2022.09.017

Wang, L. J., Wang, X. M., Chang, J., Wang, P., Liu, C. Q., Yuan, L., Yin, Q. Q., Zhu, Q., & Lu, F. S. (2022). Effect of the combined compound probiotics with glycyrrhinic acid on alleviating cytotoxicity of IPEC-J2 cells induced by multi-mycotoxins. *Toxins, 14*(10), 670. https://doi.org/10.3390/toxins14100670

Wang, Q. X., Huang, Y. W., Li, Y., Zhang, L. Y., Tang, H., Zhang, J. Z., Cheng, G. Q., Zhao, M. H., Lu, T. M., Zhang, Q., Luo, P., Zhu, Y. H., Xia, F., Zhang, Y., Liu, D. D., Wang, C., Li, H. Y., Qiu, C., Wang, J. G., & Guo, Q. Y. (2022). Glycyrrhizic acid mitigates tripterygium-glycoside-tablet-induced acute liver injury via PKM2 regulated oxidative stress. *Metabolites, 12*(11), 1128. https://doi.org/10.3390/metabo12111128

Wang, S., Wu, K. T., Xue, D. F., Zhang, C., Rajput, S. A., & Qi, D. S. (2021). Mechanism of deoxynivalenol mediated gastrointestinal toxicity: Insights from mitochondrial dysfunction. *Food and Chemical Toxicology, 153*, Article 112214. https://doi.org/10.1016/j.fct.2021.112214

Woelflingseder, L., Del Favero, G., Blazevic, T., Heiss, E. H., Haider, M., Warth, B., Adam, G., & Marko, D. (2018). Impact of glutathione modulation on the toxicity of the *Fusarium* mycotoxins deoxynivalenol (DON), NX-3 and butenolide in human liver cells. *Toxicology Letters, 299*, 104–117. https://doi.org/10.1016/j.toxlet.2018.09.007

Xu, X. X., Chang, J., Wang, P., Liu, C. Q., Liu, M. J., Zhou, T., Yin, Q. Q., & Yan, G. R. (2023). Combination of glycyrrhizic acid and compound probiotics alleviates deoxynivalenol-induced damage to weaned piglets. *Ecotoxicology and Environmental Safety, 256*, Article 114901. https://doi.org/10.1016/j.ecoenv.2023.114901

Xu, X. X., Chang, J., Wang, P., Liu, C. Q., Zhou, T., Yin, Q. Q., & Yan, G. R. (2023). Glycyrrhinic acid and probiotics alleviate deoxynivalenol-induced cytotoxicity in intestinal epithelial cells. *AMB Express, 13*(1), 52. https://doi.org/10.1186/s13568-023-01564-5

Xu, X. X., Chang, J., Wang, P., Yin, Q. Q., Liu, C. Q., Li, M. L., Song, A. D., Zhu, Q., & Lu, F. S. (2020). Effect of chlorogenic acid on alleviating inflammation and apoptosis of IPEC-J2 cells induced by deoxyniyalenol. *Ecotoxicology and Environmental Safety, 205*, Article 111376. https://doi.org/10.1016/j.ecoenv.2020.111376

Yang, Y. X., Yu, S., Jia, B. X., Liu, N., & Wu, A. (2020). Metabolomic profiling reveals similar cytotoxic effects and protective functions of quercetin during deoxynivalenol- and 15-acetyl deoxynivalenol-induced cell apoptosis. *Toxicology in Vitro, 66*, Article 104838. https://doi.org/10.1016/j.tiv.2020.104838

Yu, M., Chen, L. K., Peng, Z., Wang, D., Song, Y. D., Wang, H. Y., Yao, P., Yan, H., Nüssler, A. K., Liu, L. G., & Yang, W. (2017). Embryotoxicity caused by DON-induced oxidative stress mediated by Nrf2/HO-1 pathway. *Toxins, 9*(6), 188. https://doi.org/10.3390/toxins9060188

Yuan, T. J., Wang, J., Chen, L. T., Shan, J. J., & Di, L. Q. (2019). Glycyrrhizic acid improving the liver protective effect by restoring the composition of *Lactobacillus*. *Journal of Functional Foods, 52*, 219–227. https://doi.org/10.1016/j.jff.2018.11.001

Zhang, J., Guo, J. F., Yang, N. N., Huang, Y., Hu, T. T., & Rao, C. L. (2022). Endoplasmic reticulum stress-mediated cell death in liver injury. *Cell Death & Disease, 13*(12), 1051. https://doi.org/10.1038/s41419-022-05444-x

Zhang, Q., Zhang, Y. L., Liu, S. S., Wu, Y. Z., Zhou, Q., Zhang, Y. Z., Zheng, X., Han, Y., Xie, C., & Liu, N. L. (2021). Adsorption of deoxynivalenol by pillared montmorillonite. *Food Chemistry, 343*, Article 128391. https://doi.org/10.1016/j.foodchem.2020.128391

Zhang, X. L., Wang, L., Zhang, H. T., Tu, F., Qiang, Y., & Nie, C. F. (2019). Decreased expression of ZO-1 is associated with tumor metastases in liver cancer. *Oncology Letters, 17*(2), 1859–1864. https://doi.org/10.3892/ol.2018.9765

Zhao, L., Zhang, L., Xu, Z. J., Liu, X. D., Chen, L. Y., Dai, J. F., Karrow, N. A., & Sun, L. (2021). Occurrence of aflatoxin B_1, deoxynivalenol and zearalenone in feeds in China during 2018–2020. *Journal of Animal Science and Biotechnology, 12*(1), 74. https://doi.org/10.1186/s40104-021-00603-0

Zhu, C., Liang, S. J., Zan, G. X., Wang, X. F., Gao, C. Q., Yan, H. C., Wang, X. Q., & Zhou, J. Y. (2023). Selenomethionine alleviates DON-induced oxidative stress via modulating Keap1/Nrf2 signaling in the small intestinal epithelium. *Journal of Agricultural and Food Chemistry, 71*(1), 895–904. https://doi.org/10.1021/acs.jafc.2c07885

Zong, Q. F., Qu, H., Zhao, Y. H., Liu, H. Y., Wu, S. L., Wang, S., Bao, W. B., & Cai, D. M. (2022). Sodium butyrate alleviates deoxynivalenol-induced hepatic cholesterol metabolic dysfunction via RORγ-mediated histone acetylation modification in weaning piglets. *Journal of Animal Science and Biotechnology, 13*(1), 133. https://doi.org/10.1186/s40104-022-00793-1